Hindawi Publishing Corporation
International Journal of Photoenergy
Volume 2012, Article ID 174862, 8 pages
doi:10.1155/2012/174862

Research Article

Simultaneous Elimination of Formaldehyde and Ozone Byproduct Using Noble Metal Modified TiO_2 Films in the Gaseous VUV Photocatalysis

Pingfeng Fu,[1] Pengyi Zhang,[2] and Jia Li[2]

[1] *School of Civil and Environment Engineering, University of Science and Technology Beijing, 30 Xueyuan Road, Haidian District, Beijing 100083, China*
[2] *State Key Joint Laboratory of Environment Simulation and Pollution Control, School of Environment, Tsinghua University, Beijing 100084, China*

Correspondence should be addressed to Pengyi Zhang, zpy@tsinghua.edu.cn

Received 30 January 2012; Accepted 16 March 2012

Academic Editor: Baibiao Huang

Simultaneous removal of low concentration formaldehyde (HCHO) and ozone byproduct was investigated in the gaseous VUV (vacuum ultraviolet) photocatalysis by using noble metal modified TiO_2 films. Noble metal (Pt, Au, or Pd) nanoparticles were deposited on TiO_2 films with ultrafine particle size and uniform distribution. Under 35 h VUV irradiation, the HCHO gas (ca. 420 ppbv) was dynamically degraded to a level of 10~45 ppbv without catalyst deactivation, and over 50% O_3 byproduct was *in situ* decomposed in the reactor. However, under the same conditions, the outlet HCHO concentration remained at 125~178 ppbv in the $O_3 + UV_{254\,nm}$ photocatalysis process and 190~260 ppbv in the $UV_{254\,nm}$ photocatalysis process. And the catalyst deactivation also appeared under $UV_{254\,nm}$ irradiation. Metallic Pt or Au could simultaneously increase the elimination of HCHO and ozone, but the PdO oxide seemed to inhibit the HCHO oxidation in the $UV_{254\,nm}$ photocatalysis. Deposition of metallic Pt or Au reduces the recombination of h^+/e^- pairs and thus increases the HCHO oxidation and O_3 reduction reactions. In addition, adsorbed O_3 may be partly decomposed by photogenerated electrons trapped on metallic Pt or Au nanoparticles under UV irradiation.

1. Introduction

The heterogeneous photocatalytic oxidation (PCO) can eliminate various kinds of volatile organic compounds (VOCs) with the potential to improve indoor air quality (IAQ) [1–4]. However, the low degradation rate [2, 5] and possible photocatalyst deactivation [6, 7] limit its practical application. Vacuum ultraviolet (VUV) with high-energy photon can dissociate oxygen and water molecules in the gas phase to reactive oxygen species such as $O(^1D)$, $O(^3P)$, and hydroxyl radicals ($^\bullet OH$) [8, 9]. Recently, several authors reported that VUV photocatalysis (i.e., TiO_2 photocatalyst combined with 185 nm VUV) showed higher decomposition rates of VOCs than the common $UV_{254\,nm}$ photocatalysis [8–12]. Furthermore, the catalyst deactivation is alleviated by effective decomposition of nonvolatile oxidation intermediates on catalyst surface [8–10]. However, ozone byproduct at a ppm level is also formed in the gaseous VUV photocatalysis [9, 10]. As ozone is also a hazardous contaminant in indoor environment, the elimination of ozone byproduct is necessary for the safe use of VUV photocatalytic technique.

Ozone-decomposing catalysts (e.g., MnO_2) have been employed to remove ozone byproduct in a separate unit following the photocatalytic process [8, 10]. However, these catalysts usually lose activity while the humidity is high [13, 14]. Besides the thermal decomposition process, the semiconductor photocatalysis has also been considered to remove gaseous ozone [15, 16]. Modification of TiO_2 with noble metals (e.g., Pt, Ag, Au) can remarkably increase the decomposition rate of ozone by trapping photogenerated electrons with metal nanoparticles [17–19]. Therefore, to eliminate ozone byproduct in this case, it is an effective way to *in situ* photocatalytically decompose O_3 via increasing the reactivity of used photocatalysts. The aim of this study is to evaluate

the feasibility of simultaneous elimination of formaldehyde and ozone byproduct in the VUV photocatalysis by using noble metal (Pt, Au, or Pd) modified TiO_2 film photocatalysts.

2. Experimental

Noble metal nanoparticles (NPs) modified TiO_2 films, that is, Pt-TiO_2, Au-TiO_2, or Pd-TiO_2 films supported on Ti mesh, were prepared via a low-temperature electrostatic self-assembly method as described in our previous paper [20]. The morphologies of the photocatalysts were observed using an ultra-high-resolution field-emission scanning electron microscope (FESEM, S-5500, Hitachi). X-ray diffraction (XRD) analysis was carried out with a Rigaku D/max-RB using Cu Kα radiation. To analyze the crystalline structure of loaded noble metal nanoparticles, the amount of deposited Pt, Au, or Pd nanoparticles reached ca. 4% (wt).

The used VUV lamp (3 W) was an ozone-producing low-pressure mercury lamp with λ_{max} at 254 nm and a minor emission (ca. 5%) at 185 nm. Two VUV lamps were located at the center of the flow photoreactor with an effective volume of 0.628 L. Two pieces of Pt (Au, Pd)-TiO_2/Ti (or TiO_2/Ti) mesh were, respectively, fixed at both sides of the lamp. The $UV_{254\,nm}$ intensity at the photocatalyst surface was 3.2 mW/cm^2. The effective residence time of HCHO gas was 21 s in the reactor with the gas-solid contact time of 0.34 s. Because the indoor formaldehyde concentration usually lies at a ppbv level, typically less than 300 ppbv [21], the inlet concentration of HCHO was set at ca. 420 ppbv. After the HCHO concentration reached dynamical equilibrium (2 h), two VUV lamps were turned on to start the 35 h VUV photocatalysis. To carry out the O_3 enhanced $UV_{254\,nm}$ (O_3 + $UV_{254\,nm}$) photocatalysis, two $UV_{254\,nm}$ lamps (3 W) were used, and the HCHO gas mixed with O_3 was introduced. The concentration (ca. 22.5 mg/m^3) of introduced O_3 is close to that of ozone generated by two VUV lamps. The other procedures were as same as the VUV photocatalytic experiments. The 35 h $UV_{254\,nm}$ photocatalysis was carried out with the same procedure except no ozone is mixed with HCHO gas. The O_3 concentration was monitored with an on-line O_3 analyzer (Model 49i, Thermo Electron). The formaldehyde concentration was analyzed by MBTH method (GB/T18204.28, China). Because the ozone may disturb the formaldehyde analysis with MBTH method, a KI (potassium iodide) coated annular denuder was used to scrub ozone while sampling.

In this study, the removal rate of HCHO and O_3 was calculated according to (E1) and (E2), and the reaction rate (R) of HCHO oxidation was calculated with (E3):

$$\text{Removal rate of HCHO} = \frac{[\text{HCHO}]_{\text{initial}} - [\text{HCHO}]_{\text{steady}}}{[\text{HCHO}]_{\text{initial}}} \times 100\%, \quad \text{(E1)}$$

$$\text{Removal rate of } O_3 = \frac{[O_3]_{\text{initial}} - [O_3]_{\text{steady}}}{[O_3]_{\text{initial}}} \times 100\%, \quad \text{(E2)}$$

$$R = \frac{Q \times \left([\text{HCHO}]_{\text{initial}} - [\text{HCHO}]_{\text{steady}}\right)}{V} \times 100\%, \quad \text{(E3)}$$

where the $[\text{HCHO}]_{\text{initial}}$ was the equilibrium concentration of HCHO before irradiation, the $[\text{HCHO}]_{\text{steady}}$ was the steady-state concentration of HCHO under UV irradiation; $[O_3]_{\text{initial}}$ represented the outlet concentration of VUV generated ozone (without photocatalysts) with a value of 22.5 mg/m^3, and the $[O_3]_{\text{steady}}$ was the steady-state concentration of ozone under UV irradiation; Q was the flow rate of HCHO gas (m^3/min), and V was the effective volume of the photoreactor (m^3).

3. Results and Discussion

3.1. Characterization of Pt (Au, Pd)-TiO_2 Film Photocatalysts. Figure 1 shows the ultra-high-resolution FESEM images of Pt, Au, and Pd modified TiO_2 films. Noble metal (Pt, Au, Pd) nanoparticles (NPs) are physically separated and uniformly dispersed on TiO_2 films with an interparticle spacing of 5~20 nm. The average particle size of loaded Pt, Au, and Pd NPs is 1.9 nm, 4.2 nm, and 3.9 nm, respectively. Each TiO_2 particle is coated with nearly 2~3 metal NPs. The surface density of noble metal NPs reaches (5~10) $\times$ 10^{11} particles per cm^2. It is obvious that noble metal NPs can be well deposited on TiO_2 films in the electrostatic self-assembly process.

The XRD analysis (Figure 2) reveals that TiO_2 films have mixed crystalline phases with 62.5% anatase and 37.5% rutile. As shown in Figure 2, the diffraction peaks at 2θ = 39.9°, 46.4°, 67.5°, and 81.3° can be attributed to the (111), (200), (220), and (311) reflections of metallic Pt (JCPDS number 4-0802). For the Au-TiO_2 films, the diffraction peaks at 2θ = 38.3°, 44.4°, 64.7°, 77.5°, and 81.9° can be attributed to the (111), (200), (220), (311), and (222) reflections of metallic Au (JCPDS number 65-8601). For the Pd-TiO_2 films, the peaks at 2θ = 33.9°, 41.9°, 60.3°, 60.9°, and 71.5° can be attributed to the (101), (110), (103), (200), and (202) reflections of palladium oxide (PdO, JCPDS number 41-1107), respectively. After annealed in air at 300°C for 1.5 h, Pt and Au NPs are still in metallic form, while Pd NPs have been oxidized to palladium oxide (PdO).

3.2. VUV Photocatalytic Degradation of Formaldehyde and Simultaneous Removal of Ozone Byproduct. As shown in Figure 3, the HCHO can be rapidly decomposed under VUV irradiation even without the photocatalyst, but ozone byproduct with high concentration (ca. 22.4 mg/m^3) appears. Abundant reactive oxygen species such as hydroxyl radical, O(^{1}D), and O(^{3}P) are formed under 185 nm VUV irradiation. So the VUV photolysis (VUV photochemical process) of HCHO can effectively occur. While TiO_2 or noble metal modified TiO_2 photocatalysts are presented, the reaction rate of HCHO decomposition increases from 1.16 to above 1.4 mg/m^3·min. The outlet concentration of residual HCHO lowers enough to 10~45 ppbv (Table 1). These steady-state HCHO concentrations are much lower than the WHO guideline level of indoor formaldehyde (80 ppbv).

Table 1: The outlet concentration and removal rates of HCHO and O_3, and reaction rates of HCHO in the 35 h VUV, $O_3 + UV_{254\,nm}$, and $UV_{254\,nm}$ photocatalysis, respectively.

Kinds of photocatalysis	Photocatalysts	Formaldehyde			Ozone	
		Concentration (ppbv)	Removal rate (%)	Reaction rate ($mg/m^3 \cdot min$)	Concentration (mg/m^3)	Removal rate (%)
VUV photocatalysis	VUV photolysis	122.4	72.9	1.16	22.4	0
	TiO_2	36.1	91.4	1.34	19.2	14.3
	Pd-TiO_2	20.1	95.3	1.43	14.2	36.6
	Pt-TiO_2	9.5	97.7	1.47	10.7	52.2
	Au-TiO_2	27.6	93.6	1.41	15.1	32.6
$O_3 + UV_{254\,nm}$ photocatalysis	TiO_2	178.8	57.4	0.85	13.8	37.8
	Pd-TiO_2	150.1	65.7	0.96	9.3	58.1
	Pt-TiO_2	125.1	68.6	1.01	6.2	72.1
	Au-TiO_2	130.6	68.8	1.02	10.8	51.4
$UV_{254\,nm}$ photocatalysis	TiO_2	263.4	37.8	0.57		
	Pd-TiO_2	251.3	37.6	0.56		
	Pt-TiO_2	190.6	56.7	0.89		
	Au-TiO_2	218.1	45.2	0.63		

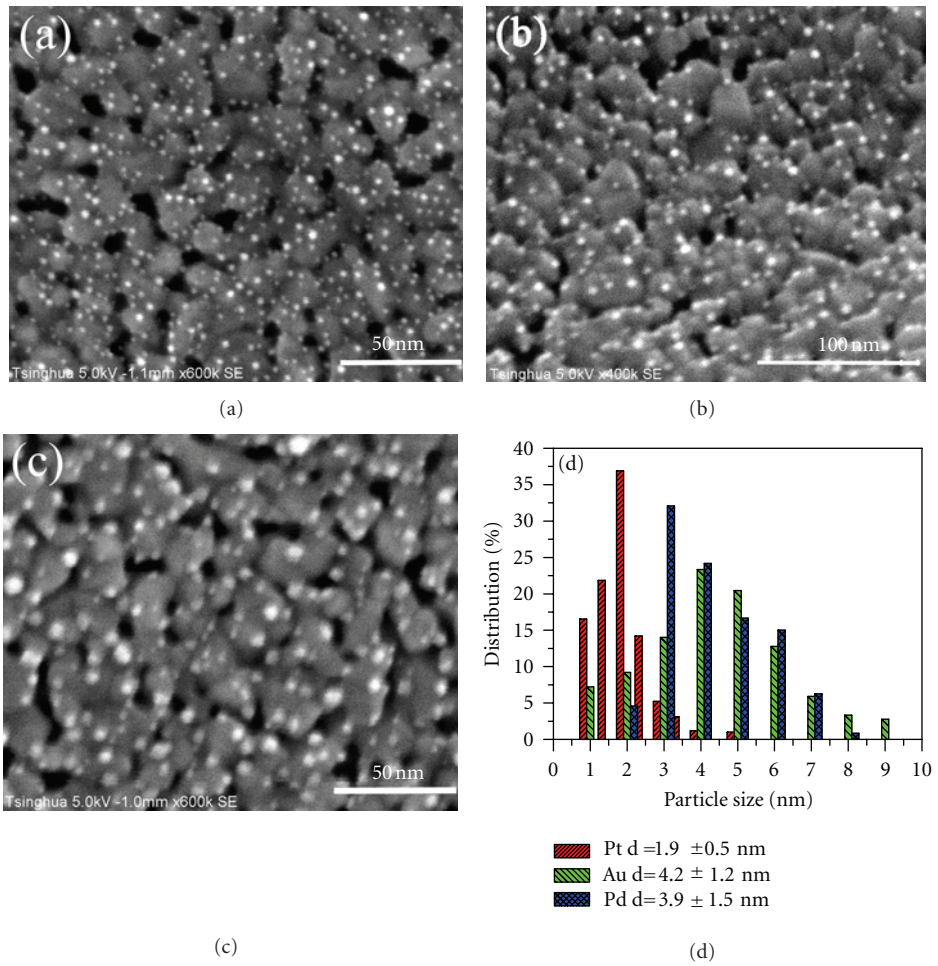

Figure 1: FESEM images of deposited Pt (a), Au (b), and Pd (c) nanoparticles on TiO_2 films. (d) The size distribution histogram of deposited Pt, Au, and Pd nanoparticles.

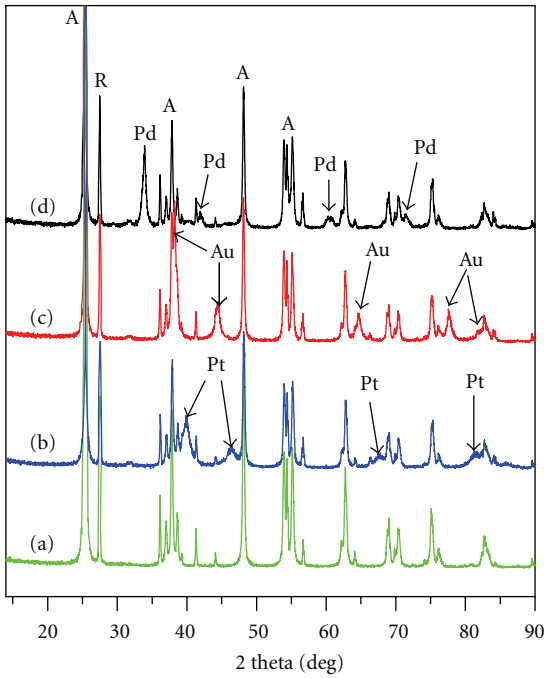

FIGURE 2: XRD patterns of as-prepared TiO_2 films (a), Pt-TiO_2 (b), Au-TiO_2 (c), and Pd-TiO_2 (d) nanocomposite films scratched from Ti wire net.

In the VUV photocatalysis, the HCHO can be decomposed both in gas phase via VUV photochemical process and on the photocatalyst surface via $UV_{254\,nm}$ excited photocatalysis [8–10]. So the presence of photocatalysts under VUV irradiation can remarkably increase the oxidation rate of VOCs. However, in the VUV photocatalysis of HCHO, only minor improvement of HCHO removal is observed by modifying TiO_2 films with noble metals. This may be attributed to that most of HCHO molecules are decomposed in gas phase not on the photocatalyst surface.

However, the removal ratio of ozone byproduct increases from 14.3% (TiO_2) to 32~52% (Au, Pd, or Pt-TiO_2) with an enhancement of 2.3~3.6-folds (Table 1). At the same time, the outlet O_3 concentration can keep almost at a same level for a long steady-state period for noble metal modified TiO_2, but it gradually rises in the case of pure TiO_2. The result suggests that ozone byproduct can be *in situ* photocatalytically decomposed in the photoreactor, and modification of TiO_2 films with noble metals can both enhance the photodegradation of O_3 and alleviate the catalyst deactivation. The results reveal that simultaneous removal of low concentration HCHO and O_3 byproduct is surly feasible in the VUV photocatalysis when TiO_2 films are modified with Pt, Au, or Pd NPs.

3.3. Comparison of HCHO Degradation in Long-Term VUV Photocatalysis, O_3 + $UV_{254\,nm}$ Photocatalysis and $UV_{254\,nm}$ Photocatalysis. Figures 4(a) and 5 show the outlet concentrations of HCHO versus irradiation time in the O_3 + $UV_{254\,nm}$ and $UV_{254\,nm}$ photocatalysis, respectively. As shown in Figures 4(a) and 5 and Table 1, the outlet concentration of HCHO reaches 125~178 ppbv in the O_3 + $UV_{254\,nm}$ photocatalysis and 190~260 ppbv in the $UV_{254\,nm}$ photocatalysis, while it is just 10~45 ppbv in the VUV photocatalysis when the same photocatalyst is used. The reaction rate of HCHO oxidation in the VUV photocatalysis is ca. 1.4 times and 2 times higher than that in the O_3 + $UV_{254\,nm}$ and $UV_{254\,nm}$ photocatalysis, respectively. As listed in Table 1, the HCHO degradation rate in the VUV photolysis (without photocatalyst) has been much higher than that in the O_3 + $UV_{254\,nm}$ or $UV_{254\,nm}$ photocatalysis. Obviously, the VUV photochemical process in gas phase makes great contribution in the oxidation of HCHO molecules in the VUV photocatalysis.

Additionally, the stability of the outlet HCHO concentration in the long-term VUV photocatalysis is also very different from that in the O_3 + $UV_{254\,nm}$ or $UV_{254\,nm}$ photocatalysis. The HCHO concentration gradually rises up, while the reaction time exceeds 25 h in the O_3 + $UV_{254\,nm}$ or $UV_{254\,nm}$ photocatalysis (Figures 4(a) and 5), while it remains at a very low level in the VUV photocatalysis (Figure 3). Due to the lower degradation rate of HCHO in the O_3 + $UV_{254\,nm}$ or $UV_{254\,nm}$ photocatalysis, the reaction intermediates combined with adsorbed HCHO molecules may persistently accumulate on the catalyst surfaces, which leads to observed catalyst deactivation. Nevertheless, the degradation behaviour under VUV irradiation suggests that no catalyst deactivation occurs in the VUV photocatalysis regardless of modification of TiO_2. Due to abundant reactive species generated in gas phase, the oxidation of reaction intermediates and HCHO should been significantly enhanced under VUV irradiation. Therefore, the carbon accumulation on the catalyst could be alleviated even the HCHO gas is continuously introduced with very short residence time. The results in this study are highly consistent with the previously observed long lifetime of the photocatalysts under VUV irradiation [8–10].

While the HCHO concentration is at a typical indoor level, the film-diffusional resistance at the interface of gas phase and catalyst film becomes very large, leading to remarkable decrease of HCHO degradation rate in the $UV_{254\,nm}$ photocatalysis [22]. Until now, it is still a great challenge for $UV_{254\,nm}$ photocatalysis using semiconductor films to effectively decompose low concentration HCHO, while the gas residence time becomes short enough to several seconds [22–24]. In this study, the results indicate that the VUV photocatalysis cannot only rapidly decompose HCHO vapor with low concentration but also avoid the deactivation of the photocatalysts. Therefore, it can be anticipated that the VUV photocatalysis is an alternative method to efficiently decompose indoor VOCs.

3.4. Enhanced Effects of Deposited Noble Metals on the Decomposition of HCHO and Ozone. As shown in Table 1, deposition of noble metals (Pt or Au) on TiO_2 surface actually increases the decomposition rate of HCHO in the VUV,

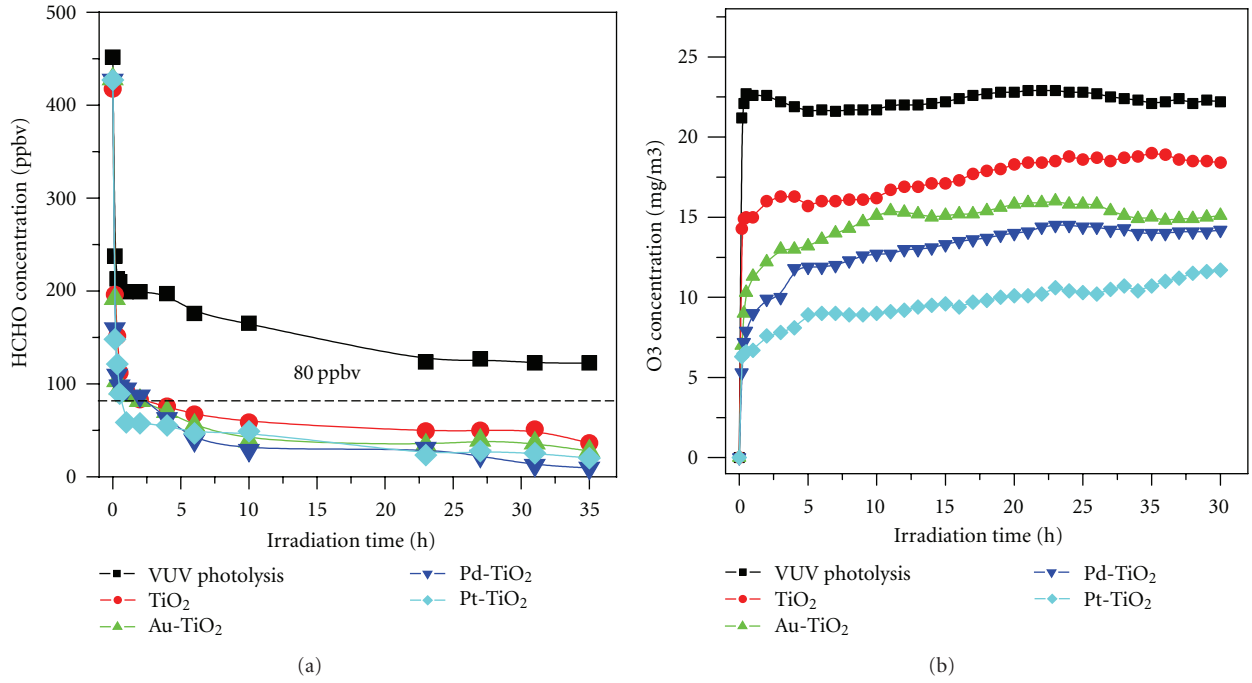

FIGURE 3: Time courses for the outlet concentration of HCHO (a) and ozone byproduct (b) with irradiation time in the 35 h VUV photocatalysis. The VUV photolysis is the VUV photochemical process without the photocatalyst.

O_3 + $UV_{254\,nm}$ or $UV_{254\,nm}$ photocatalysis. For the ozone decomposition, all of these three noble metal NPs (Pt, Au, or Pd) can have evident positive role. Especially, the removal ratio of HCHO increases from 57.4% (TiO_2) to ca. 68% (Pt, or Au-TiO_2) and that of O_3 augments from 37.8% (TiO_2) to 72.1% (Pt-TiO_2) in the O_3 + $UV_{254\,nm}$ photocatalysis. In the $UV_{254\,nm}$ photocatalysis, the reaction rate of HCHO oxidation increases from 0.57 mg/m^3·min (TiO_2) to 0.89 mg/m^3·min (Pt-TiO_2). However, deposition of Pd NPs in form of PdO seems to be deleterious to HCHO oxidation in the $UV_{254\,nm}$ photocatalysis (Figure 5).

These results indicate that deposited metallic NPs (Pt, Au) can enhance the photocatalytic decomposition of both HCHO and O_3 molecules. While the PdO NPs appears, photocatalytic oxidation of HCHO is inhibited, but the ozone decomposition surely enhanced. The O_3 removal behaviours (Figures 3 and 4) also reveal that the ozone, *in situ* generated in the VUV photoreactor or exteriorly added, can be effectively decomposed similarly. In the tested noble NPs (Au, Pt, or Pd), the metallic Pt NPs modified TiO_2 exhibits the highest activity in the HCHO oxidation and O_3 reduction reactions. In addition, it can find that noble metal deposition has much more evident effect in O_3 removal than in the HCHO degradation.

3.5. Proposed Mechanism of Positive Role of Deposited Noble Metallic NPs. In this work, the thermal decomposition of O_3 on noble metal modified TiO_2 films is proved to be little (less than 5%) at room temperature in the dark. So the observed O_3 decomposition should be ascribed to heterogeneous photodegradation. Therefore, we propose the mechanism of enhanced electron-hole separation caused by deposited noble metallic Pt or Au NPs and O_3 decomposition routes (Figure 6). As presented in Figure 6, locally formed metallic Pt or Au NPs act as the electron trapping center. When the photogenerated electrons are trapped by metallic Pt or Au, electron-hole pairs are efficiently separated, producing more $^{\bullet}OH$ on the TiO_2 surface [20, 25–28]. Thus, the photocatalytic oxidation of HCHO is significantly enhanced.

For the photocatalytic decomposition of O_3, the previous ESR measurements revealed that ozonide radical anion ($O_3^{\bullet-}$), surface $O^{\bullet-}$ radicals, and hydroperoxyl radical ($HO_2^{\bullet}$) could be produced at the gaseous O_3/TiO_2 interface under UV irradiation [29]. Therefore, we propose the photocatalytic decomposition of O_3 on exposed TiO_2 surface of the Pt-TiO_2 (or Au-TiO_2) as follows [15, 29, 30]:

$$O_3 + e^- \longrightarrow O_3^{\bullet-} \quad \text{(R1)}$$

$$O_3^{\bullet-} \xrightarrow{h\nu} O_2 + O^{\bullet-} \quad \text{(R2)}$$

$$O^{\bullet-} + H_2O \longrightarrow OH^- + {}^{\bullet}OH \quad \text{(R3)}$$

$$O_3^{\bullet-} + H_2O \longrightarrow OH^- + {}^{\bullet}OH + O_2 \quad \text{(R4)}$$

$$O_2 + e^- \longrightarrow O_2^{\bullet-} \quad \text{(R5)}$$

$$O_2^{\bullet-} + O_3 \longrightarrow {}^{\bullet}OH + O_3^{\bullet-} \quad \text{(R6)}$$

The adsorbed O_3 is reduced to $O_3^{\bullet-}$ radicals by capturing the photogenerated electrons (R1). Under UV irradiation, the unstable $O_3^{\bullet-}$ radicals rapidly split to form O_2 and $O^{\bullet-}$ radicals (R2). Then, the adsorbed water molecules are oxidized by $O_3^{\bullet-}$ or $O^{\bullet-}$ radicals to form $^{\bullet}OH$ radicals (R3) and

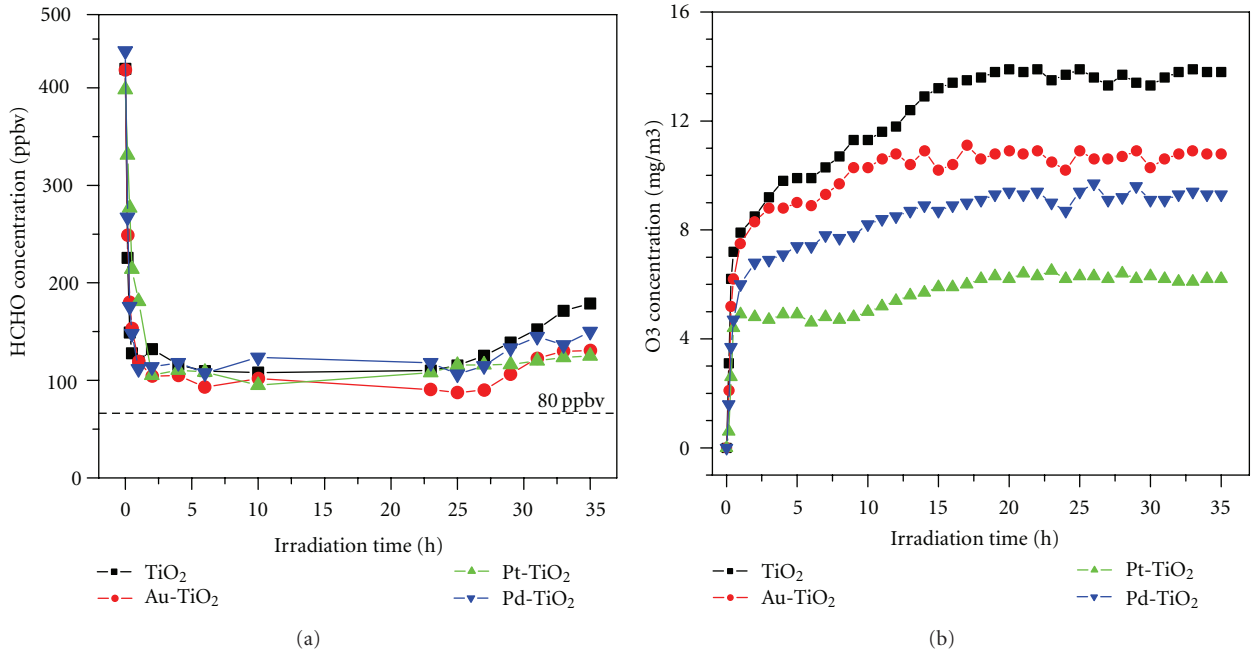

Figure 4: Time courses for the outlet concentration of formaldehyde (a) and ozone (b) with irradiation time in the 35 h O_3 + $UV_{254\,nm}$ photocatalysis.

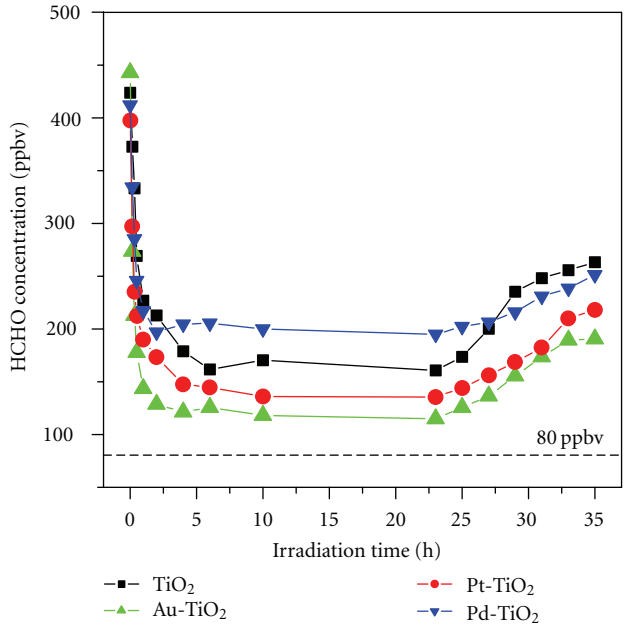

Figure 5: Time courses for the outlet concentration of formaldehyde with irradiation time in the 35 h $UV_{254\,nm}$ photocatalysis.

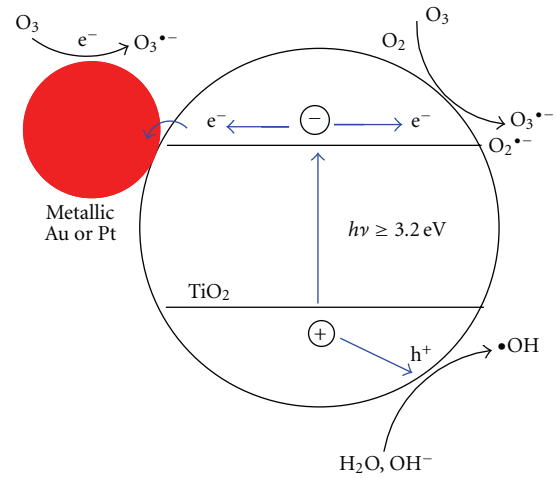

Figure 6: Proposed mechanism of enhanced electron-hole separation caused by deposited noble metallic Au or Pt nanoparticles and O_3 decomposition routes on the Pt or Au modified TiO_2.

(R4). Alternatively, adsorbed O_2 will also capture electrons, leading to formation of $^{\bullet}OH$ and $O_3^{\bullet-}$ radicals (R5) and (R6). Obviously, enhanced separation of h^+/e^- pairs allows more photogenerated electrons to be captured by adsorbed O_3 molecules.

As shown in Table 1, the O_3 removal rate is improved over 2 times with metallic Pt or Au modified TiO_2. The enhanced h^+/e^- separation efficiency by deposited Pt or Au NPs could improve the photocatalytic decomposition of adsorbed O_3 on exposed TiO_2. But it should be noted that the exposed TiO_2 surface area, available for O_3 decomposition, is also remarkably reduced owing to covering Pt or Au NPs layer. Since the ESR tests have proved that adsorbed O_3 can capture electrons to form $O_3^{\bullet-}$ radicals on CeO_2 [31] or TiO_2 [29] surface even in the dark. We propose here that adsorbed O_3 may also interact with electron-rich surface sites on Pt or Au NPs to form $O_3^{\bullet-}$ radicals (R1) by considering the fact that photogenerated electrons have been readily trapped

by metallic Pt or Au NPs. With the help of UV irradiation, the split of $O_3^{\bullet -}$ radicals on Pt or Au NPs is enhanced (R2). The similar phenomenon had been observed in the ESR test of gaseous O_3/TiO_2 interface [29]. Then, the chain radical reactions proceeded on Pt or Au NPs may be similar to those on UV-irradiated TiO_2 (R3) and (R4).

4. Conclusions

In this work, we investigated the feasibility of simultaneous elimination of gaseous formaldehyde and ozone byproduct in the VUV photocatalysis process. The gaseous HCHO with the inlet concentration of ca. 420 ppbv can be readily degraded to meet the WHO guideline level of indoor formaldehyde in a short solid-gas contact time (0.34 s). However, the O_3 + $UV_{254\,nm}$ or $UV_{254\,nm}$ photocatalysis shows much lower removal ratio of HCHO with observable catalyst deactivation. By modifying TiO_2 film with noble metallic Pt or Au, both HCHO removal and ozone decomposition are significantly improved. Especially, over 50% ozone byproduct can be *in situ* decomposed by using Pt-TiO_2 films. However, deposition of PdO oxide seems to inhibit the oxidation of HCHO in the $UV_{254\,nm}$ photocatalysis but enhances the O_3 decomposition in the VUV or O_3 + $UV_{254\,nm}$ photocatalysis. Loaded metallic Pt or Au particles reduce the recombination of h^+/e^- pairs and thus increase the HCHO oxidation and O_3 photocatalytical reduction on exposed TiO_2 surface. In addition, adsorbed O_3 may also be decomposed on electron-rich surface sites of metallic Pt or Au under UV irradiation.

Acknowledgments

The authors gratefully acknowledge the financial support from National High Technology Research and Development Program of China (2012AA062701), National Nature Science Foundation of China (50908132), and Tsinghua University Initiative Scientific Research Program.

References

[1] S. Wang, H. M. Ang, and M. O. Tade, "Volatile organic compounds in indoor environment and photocatalytic oxidation: state of the art," *Environment International*, vol. 33, no. 5, pp. 694–705, 2007.

[2] B. Y. Lee, S. W. Kim, S. C. Lee, H. H. Lee, and S. J. Choung, "Photocatalytic decomposition of gaseous formaldehyde using TiO_2, SiO_2-TiO_2 and Pt-TiO_2," *International Journal of Photoenergy*, vol. 5, no. 1, pp. 21–25, 2003.

[3] S. V. Awate, A. A. Belhekar, and S. V. Bhagwat, "Effect of gold dispersion on the photocatalytic activity of mesoporous titania for the vapor-phase oxidation of acetone," *International Journal of Photoenergy*, vol. 5, no. 1, pp. 21–25, 2003.

[4] P. Monneyron, A. De La Guardia, M. H. Manero, E. Oliveros, M. T. Maurette, and F. Benoit-Marquié, "Co-treatment of industrial air streams using A.O.P. and adsorption processes," *International Journal of Photoenergy*, vol. 5, no. 3, pp. 167–174, 2003.

[5] C. H. Ao and S. C. Lee, "Indoor air purification by photocatalyst TiO_2 immobilized on an activated carbon filter installed in an air cleaner," *Chemical Engineering Science*, vol. 60, no. 1, pp. 103–109, 2005.

[6] M. C. Blount and J. L. Falconer, "Steady-state surface species during toluene photocatalysis," *Applied Catalysis B*, vol. 39, no. 1, pp. 39–50, 2002.

[7] H. Einaga, S. Futamura, and T. Ibusuki, "Heterogeneous photocatalytic oxidation of benzene, toluene, cyclohexene and cyclohexane in humidified air: comparison of decomposition behavior on photoirradiated TiO_2 catalyst," *Applied Catalysis B*, vol. 38, no. 3, pp. 215–225, 2002.

[8] J. Jeong, K. Sekiguchi, and K. Sakamoto, "Photochemical and photocatalytic degradation of gaseous toluene using short-wavelength UV irradiation with TiO_2 catalyst: comparison of three UV sources," *Chemosphere*, vol. 57, no. 7, pp. 663–671, 2004.

[9] P. Zhang, J. Liu, and Z. Zhang, "VUV photocatalytic degradation of toluene in the gas phase," *Chemistry Letters*, vol. 33, no. 10, Article ID CL-040801, pp. 1242–1243, 2004.

[10] J. Jeong, K. Sekiguchi, W. Lee, and K. Sakamoto, "Photodegradation of gaseous volatile organic compounds (VOCs) using TiO_2 photoirradiated by an ozone-producing UV lamp: decomposition characteristics, identification of by-products and water-soluble organic intermediates," *Journal of Photochemistry and Photobiology A*, vol. 169, no. 3, pp. 279–287, 2005.

[11] J. Jeong, K. Sekiguchi, M. Saito, Y. Lee, Y. Kim, and K. Sakamoto, "Removal of gaseous pollutants with a UV-$C_{254+185\,nm}$/TiO_2 irradiation system coupled with an air washer," *Chemical Engineering Journal*, vol. 118, no. 1-2, pp. 127–130, 2006.

[12] N. Quici, M. L. Vera, H. Choi et al., "Effect of key parameters on the photocatalytic oxidation of toluene at low concentrations in air under 254+185 nm UV irradiation," *Applied Catalysis B*, vol. 95, no. 3-4, pp. 312–319, 2010.

[13] Z. Hao, D. Cheng, Y. Guo, and Y. Liang, "Supported gold catalysts used for ozone decomposition and simultaneous elimination of ozone and carbon monoxide at ambient temperature," *Applied Catalysis B*, vol. 33, no. 3, pp. 217–222, 2001.

[14] K. Sekiguchi, A. Sanada, and K. Sakamoto, "Degradation of toluene with an ozone-decomposition catalyst in the presence of ozone, and the combined effect of TiO_2 addition," *Catalysis Communications*, vol. 4, no. 5, pp. 247–252, 2003.

[15] P. Pichat, J. Disdier, C. Hoang-van, D. Mas, G. Goutailler, and C. Gaysee, "Purification /deordorization of indoor air and gas effluents by TiO_2 photocatalysts," *Catalysis Today*, vol. 63, no. 2–4, pp. 363–369, 2000.

[16] A. Mills, S. K. Lee, and A. Lepre, "Photodecomposition of ozone sensitized by a film of titanium dioxide on glass," *Journal of Photochemistry and Photobiology A*, vol. 155, no. 1-3, pp. 199–205, 2003.

[17] K. C. Cho, K. C. Hwang, T. Sano, K. Takeuchi, and S. Matsuzawa, "Photocatalytic performance of Pt-loaded TiO_2 in the decomposition of gaseous ozone," *Journal of Photochemistry and Photobiology A*, vol. 161, no. 2-3, pp. 155–161, 2004.

[18] Y. C. Lin and C. H. Lin, "Catalytic and photocatalytic degradation of ozone via utilization of controllable nano-Ag modified on TiO_2," *Environmental Progress*, vol. 27, no. 4, pp. 496–502, 2008.

[19] P. He, M. Zhang, D. Yang, and J. Yang, "Preparation of Au-loaded TiO_2 by photochemical deposition and ozone photocatalytic decomposition," *Surface Review and Letters*, vol. 13, no. 1, pp. 51–55, 2006.

[20] P. Fu and P. Zhang, "Uniform dispersion of Au nanoparticles on TiO_2 film via electrostatic self-assembly for photocatalytic

degradation of bisphenol A," *Applied Catalysis B*, vol. 96, no. 1-2, pp. 176–184, 2010.

[21] T. Salthammer, S. Mentese, and R. Marutzky, "Formaldehyde in the indoor environment," *Chemical Reviews*, vol. 110, no. 4, pp. 2536–2572, 2010.

[22] F. Shiraishi, D. Ohkubo, K. Toyoda, and S. Yamaguchi, "Decomposition of gaseous formaldehyde in a photocatalytic reactor with a parallel array of light sources: 1. Fundamental experiment for reactor design," *Chemical Engineering Journal*, vol. 114, no. 1-3, pp. 153–159, 2005.

[23] L. Yang, Z. Liu, J. Shi, Y. Zhang, H. Hu, and W. Shangguan, "Degradation of indoor gaseous formaldehyde by hybrid VUV and TiO_2/UV processes," *Separation and Purification Technology*, vol. 54, no. 2, pp. 204–211, 2007.

[24] L. Yang, Z. Liu, J. Shi, H. Hu, and W. Shangguan, "Design consideration of photocatalytic oxidation reactors using TiO_2-coated foam nickels for degrading indoor gaseous formaldehyde," *Catalysis Today*, vol. 126, no. 3-4, pp. 359–368, 2007.

[25] Z. Sheng, Z. Wu, Y. Liu, and H. Wang, "Gas-phase photocatalytic oxidation of NO over palladium modified TiO_2 catalysts," *Catalysis Communications*, vol. 9, no. 9, pp. 1941–1944, 2008.

[26] M. A. Aramendía, J. C. Colmenares, A. Marinas et al., "Effect of the redox treatment of Pt/TiO_2 system on its photocatalytic behaviour in the gas phase selective photooxidation of propan-2-ol," *Catalysis Today*, vol. 128, no. 3-4, pp. 235–244, 2007.

[27] P. Falaras, I. M. Arabatzis, T. Stergiopoulos, and M. C. Bernard, "Enhanced activity of silver modified thin-film TiO_2 photocatalysts," *International Journal of Photoenergy*, vol. 5, no. 3, pp. 123–130, 2003.

[28] A. Yamakata, T. A. Ishibashi, and H. Onishi, "Pressure dependence of electron- and hole-consuming reactions in photocatalytic water splitting on Pt/TiO_2 studied by time-resolved IR absorption spectroscopy," *International Journal of Photoenergy*, vol. 5, no. 1, pp. 7–9, 2003.

[29] M. D. Hernández-Alonso, J. M. Coronado, A. Javier Maira, J. Soria, V. Loddo, and V. Augugliaro, "Ozone enhanced activity of aqueous titanium dioxide suspensions for photocatalytic oxidation of free cyanide ions," *Applied Catalysis B*, vol. 39, no. 3, pp. 257–267, 2002.

[30] M. Nicolas, M. Ndour, O. Ka, B. D'Anna, and C. George, "Photochemistry of atmospheric dust: ozone decomposition on illuminated titanium dioxide," *Environmental Science and Technology*, vol. 43, no. 19, pp. 7437–7442, 2009.

[31] A. Naydenov, R. Stoyanova, and D. Mehandjiev, "Ozone decomposition and CO oxidation on CeO_2," *Journal of Molecular Catalysis. A, Chemical*, vol. 98, no. 1, pp. 9–14, 1995.